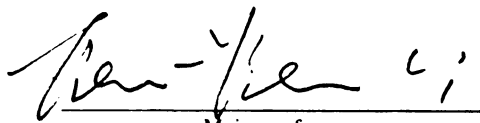This is to certify that the

dissertation entitled

On the Galerkin Method with Vector Basis Function

presented by

Hong Zhang Sun

has been accepted towards fulfillment
of the requirements for

Ph. D degree in Applied Mathematics

Major professor

Date 7-24-59

PLACE IN RETURN BOX to remove this checkout from your record.
TO AVOID FINES return on or before date due.

DATE DUE	DATE DUE	DATE DUE
_____	_____	_____
_____	_____	_____
_____	_____	_____
_____	_____	_____
_____	_____	_____
_____	_____	_____
_____	_____	_____

c:\circ\datedue.pm3-p.

ON THE GALERKIN METHOD WITH VECTOR BASIS FUNCTIONS

By

Hong Zhang Sun

A DISSERTATION

Submitted to
Michigan State University
in partial fulfillment of the requirements
for the degree of

DOCTOR OF PHILOSOPHY

Department of Mathematics

1989

ABSTRACT

ON THE GALERKIN METHOD WITH VECTOR BASIS FUNCTIONS

By

Hong Zhang Sun

The Galerkin method with new vector basis functions has been used by researchers in electrical engineering. Many experiments show that the new vector basis functions are ideally suited for representing surface electric current and surface magnetic current on the triangulated surface of the given dielectric scatterer. The efficient and simple numerical algorithms have been developed. In this work, a theoretical analysis on the convergence, error estimate and numerical stability of this method is given for a certain types of electric field integral equations. Finally, the formulation of coupled surface integral equations and corresponding matrix equation is demonstrated and numerical results are presented for the case of a homogeneous dielectric sphere.

ACKNOWLEDGEMENTS

TABLE OF CONTENTS

LIST OF FIGURES

LIST OF TABLES

INTRODUCTION

There is a very broad class of practical problems in engineering electromagnetics which are of the boundary value type for perfect electrically conducting bodies. Such problems generally require the determination of various electrical quantities for a conducting body and are called electrodynamic problems. In such problems, the current distribution is often the fundamental quantity. Knowledge of the current distribution on the body is sufficient to determine other electrical quantities such as the charge distribution, scattering pattern or radar cross-section. We usually call this type of problem a scattering problem.

A rapid expansion, both in computer capabilities and in the availability of efficient and highly stable numerical techniques, has resulted in an increasing interest in developing computer codes for treating electrodynamic problems. The most notable step in this direction is using the electric field integral equation formulations, both in the time and frequency domains, in which the body is modeled as a surface patch model. The surface patch model is easy to describe to the computer and a number of methods have been developed for two and three-dimensional scattering problems. Among them a simple efficient Galerkin procedure with two dimensional vector basis functions defined on triangular surface patches or three-dimensional vector basis functions on tetrahedral volume elements has been used by many researchers. In this work a theoretical analysis on the convergence, error estimate, and numerical stability of this procedure is given for

1

a certain types of electric field integral equations. The analysis can be applied to other types of electric field integral equations in both two-dimensional and three-dimensional cases similarly.

Usually an electric field integral equation is formulated as

$$\{ \mathbf{T} \mathbf{J}(\mathbf{r}) \}|_{\tan} = \mathbf{E}^i(\mathbf{r})|_{\tan} , \quad \mathbf{r} \in S ,$$

where $\mathbf{T}$ is a linear integral operator, $\mathbf{J}$ is an equivalent electric surface current, $\mathbf{E}^i$ is an incident electric field, and S is a regular two-dimensional region. The subscript "tan" refers to the S tangential component.

Under appropriate assumptions this integral equation is well-posed. The equation is then solved by the Galerkin method as follows:

1) Triangular elements are used to model a scattering two-dimensional body in which the electrical parameters are assumed constant in each triangular patch.

2) Special vector basis functions $\{ \mathbf{f}_n \}_{n=1}^{N}$ are defined on the triangular elements to insure that the normal electric field satisfies the correct jump condition at interfaces between different dielectric media.

3) A test function $\hat{\mathbf{J}} = \sum I_n \mathbf{f}_n$ is substituted into the integral equation to obtain $\mathbf{T} \hat{\mathbf{J}} = \mathbf{E}^i + \mathbf{ERR}$. Setting $< \mathbf{ERR} , \mathbf{f}_m > = 0$ ($m = 1, \ldots, N$), (here $<,>$ denotes the inner product for the Hilbert space under consideration), the integral equation is converted to a matrix equation:

$$\mathbf{Z}_N \mathbf{I} = \mathbf{V} ,$$

where $\mathbf{Z}_N$ is an $N \times N$ matrix with $< \mathbf{T}\mathbf{f}_n , \mathbf{f}_m >$ as its $(m, n)^{th}$ entry, $\mathbf{I} = (I_1, \ldots, I_N)^T$ is an unknown vector of coefficients of the test function $\hat{\mathbf{J}}$, and $\mathbf{V} = (< \mathbf{E}^i , \mathbf{f}_1 >, \ldots, < \mathbf{E}^i , \mathbf{f}_N >)^T$ is a known vector with $< \mathbf{E}^i , \mathbf{f}_n >$ as its nth component. Solving this system numerically, an approximate solution $\mathbf{J}_N$ of the electric field integral equation is obtained.

This work is organized as follows. Chapter 1 describes vector basis functions and their properties. In Chapter 2, the projection method (the Galerkin method is a special case) is introduced. The definition of Galerkin projection used in this work and its properties are given. Chapter 3 shows the nonsingularity of the matrix Z_N , the convergence and the error bound of the approximate solution to the exact solution. In Chapter 4, the bound of the condition number of the matrix Z_N is derived, which shows the stability of the numerical computation. In Chapter 5, the formulation of coupled surface integral equations and the corresponding matrix equation is demonstrated. Then the numerical results are presented for the case of a homogeneous dielectric sphere.

CHAPTER 1

Basis Functions

In this Chapter we describe a set of vector basis functions, originally proposed by Glisson[1], which are suitable for use with the integral equation under consideration and triangular patch modeling.

To begin with, an arbitrary two-dimensional body S in $\mathbf{R}^3$ is modeled by triangular patches. In this context, S is sometime called the *scatterer*. The body is assumed to be connected, orientable, of finite extent, and composed of non-intersecting surfaces. In general, a triangulated surface modeling an arbitrary body consists of planar triangular faces, vertices, and edges. These geometrical elements are illustrated in Fig.1. Note that real world problems are often defined over bodies with curved boundary or curved surface. They are not amenable to planar triangular modeling. In practice, we usually assume that the geometrical discretization error can be decreased by reducing the size of the elements and ignoring misfits. Eventually, we shall restrict our attention to a plate S, that can be modeled by planar triangular patches perfectly.

Once the two-dimensional scatterer has been appropriately modeled by triangular patches, the edges of the triangles are of primary importance for the development of the basis functions. Fig.2 shows two triangles, T_n^+ and T_n^-, associated with nth edge of a triangulated surface modeling a scatterer. Points in T_n^+ may be designated either by the position vector $\mathbf{r}$ with respect to the origin $\mathbf{0}$, or by the position vector $\rho_n^+ = \rho_n^+(\mathbf{r})$ defined with respect to the free vertex of T_n^+. Similar remarks apply to the position vector ρ_n^-
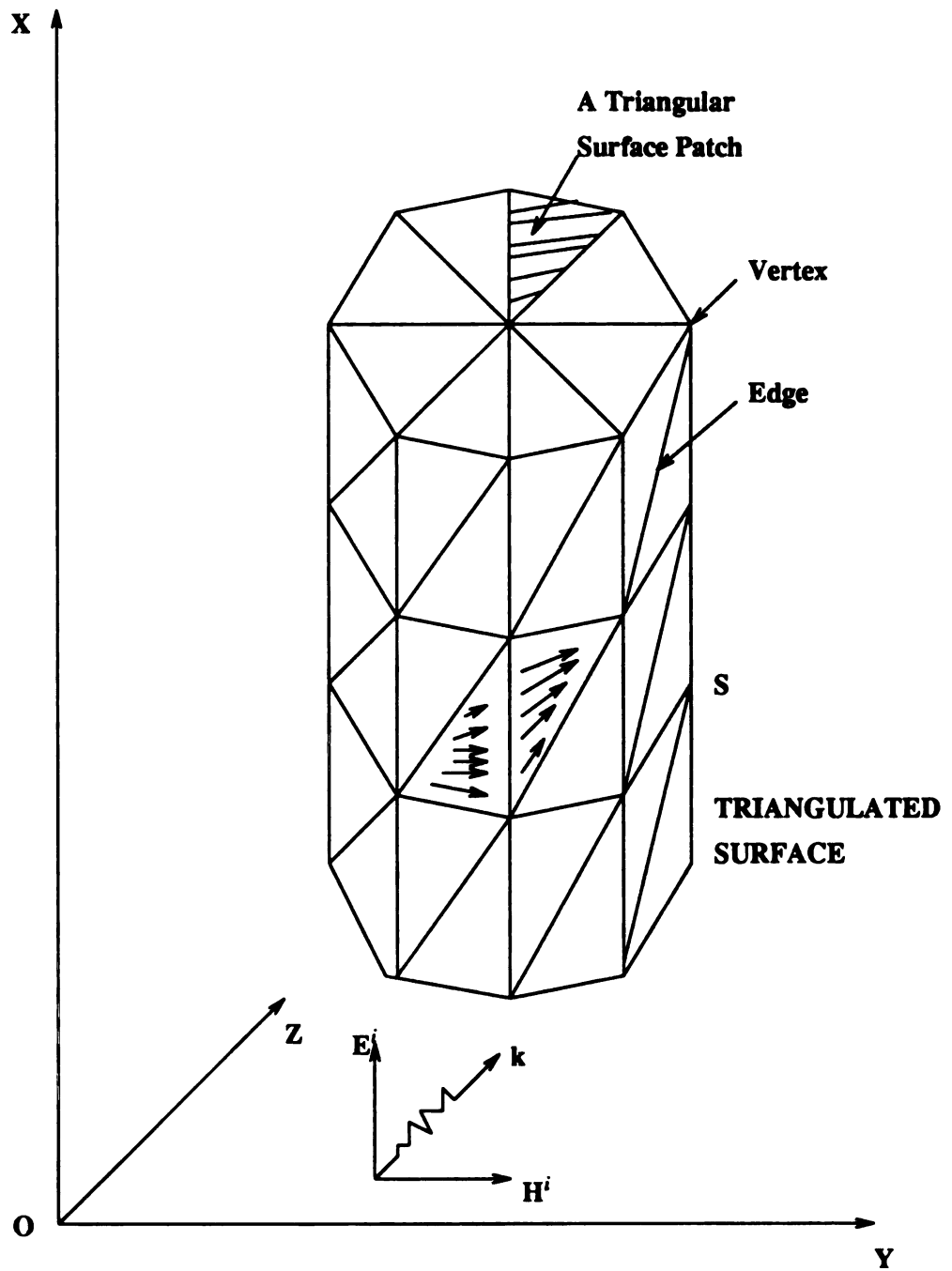
4

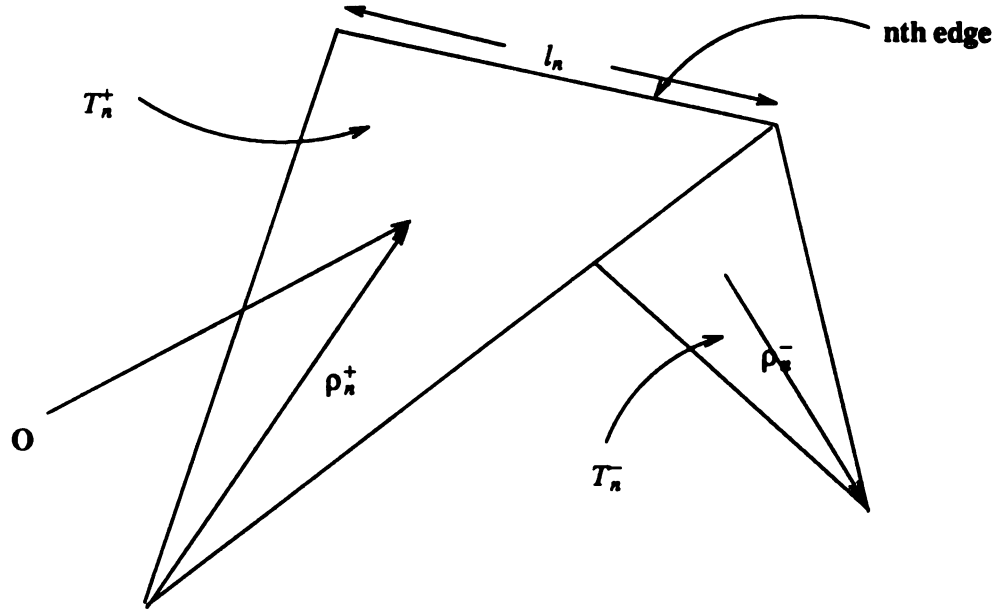Fig.1. Finite circular cylinder dielectric scatterer.

Figure 2. Local coordinates associated with an edge.

except that it is directed toward the free vertex of T_n^-. The plus or minus designation of the triangles is determined by the choice of a positive current reference direction for the nth edge which is assumed to be from T_n^+ to T_n^-. The electric current flows along the radial direction ρ_n^+ in the triangle T_n^+ and similarly flows along the radial direction ρ_n^- in the triangle T_n^-. We define a function associated with the nth edge as

$$
\mathbf{f}_n(\mathbf{r}) = \begin{cases} l_n\, \rho_n^+ / 2A_n^+ , & \text{for all } \mathbf{r} \text{ in } T_n^+ \\ l_n\, \rho_n^- / 2A_n^- , & \text{for all } \mathbf{r} \text{ in } T_n^- \text{ but not on the } n\text{th edge} \\ 0, & \text{otherwise} \end{cases} \tag{1.1}
$$

where l_n is the length of the edge and $A_n^\pm$ is the area of the triangle $T_n^\pm$. (Note that we use

the convention, followed throughout this work, that subscripts refer to edges while superscripts refer to faces). It is easy to verify that $\{$ f_i $\}$ are linearly independent. The unknown electric current can be approximated by

$$\hat{J}(r) = \sum_{n=1}^{N} I_n\, f_n(r).$$

(1.2)

The summation is over the N edges that make up the triangular model of S. The basis functions $f_n(r)$ have several properties that make them useful for representing $\hat{J}(r)$.
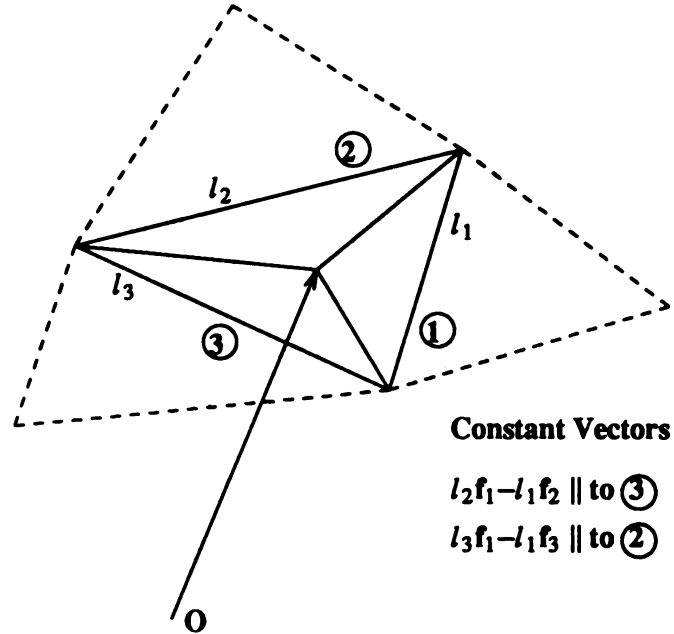

Fig.3. Three edge currents associated with a triangle.

1) Within each triangle $\hat{J}(r)$ is the sum of three basis functions that are associated with the three edges. Fig.3 shows that the superposition of the basis functions with a triangle conveniently represents a constant current flowing in an arbitrary direction

within the triangle.

2) At each edge, $f_n(\mathbf{r})$ has no component normal to that edge except at the nth edge.

3) The component of $f_n(\mathbf{r})$ normal to the nth edge is constant and continuous across the edge because the normal component of $\rho_n^{\pm}$ along the nth edge is just the height of $T_n^{\pm}$ with nth edge as the base and the height expressed as $(2A_n^{\pm})/l_n$. This latter factor normalizes $f_n(\mathbf{r})$ in (1.1) such that its flux density normal to the nth edge is unity, hence ensuring continuity of the component of $f_n(\mathbf{r})$ normal to the edge.

4) The surface divergence of the basis function is

$$
\nabla \cdot f_n(\mathbf{r}) = \begin{cases} l_n / A_n^+ , & \mathbf{r} \text{ in the interior of } T_n^+ \\ -l_n / A_n^- , & \mathbf{r} \text{ in the interior of } T_n^- \\ 0 , & \text{otherwise} \end{cases} \tag{1.3}
$$

where the surface divergence in $T_n^{\pm}$ is $(\pm 1/\rho_n^{\pm}) \, \partial(\rho_n^{\pm} f_n)/\partial\rho_n^{\pm}$ (f_n is the component of f_n in the direction of ρ_n). The charge density is thus constant in the interior of each triangle, and the basis functions for the charge evidently have the form of pulse doublets.

5) The moment of f_n is given by $(A_n^+ + A_n^-) \, f_n^{avg}$ where

$$
(A_n^+ + A_n^-) \, f_n^{avg} \equiv \int_{T_n^+ + T_n^-} f_n \, ds = \frac{l_n}{2} (\rho_n^{c+} + \rho_n^{c-}) \tag{1.4}
$$

$$
= l_n (\mathbf{r}_n^{c-} - \mathbf{r}_n^{c+})
$$

and $\rho_n^{c\pm}$ is the vector from the free vertex to the centroid of $T_n^{\pm}$ with ρ_n^{c+} directed away from the vertex and ρ_n^{c-} directed toward the vertex, as shown in Fig.4, and $\mathbf{r}_n^{c\pm}$ is the vector from the origin $\mathbf{0}$ to the centroid of $T_n^{\pm}$.

6) If edge n is on the boundary of S, then only one of the triangles, T_n^+ or T_n^-, is interior to S. In this case it is assumed that f_n is defined over only the triangle in the interior
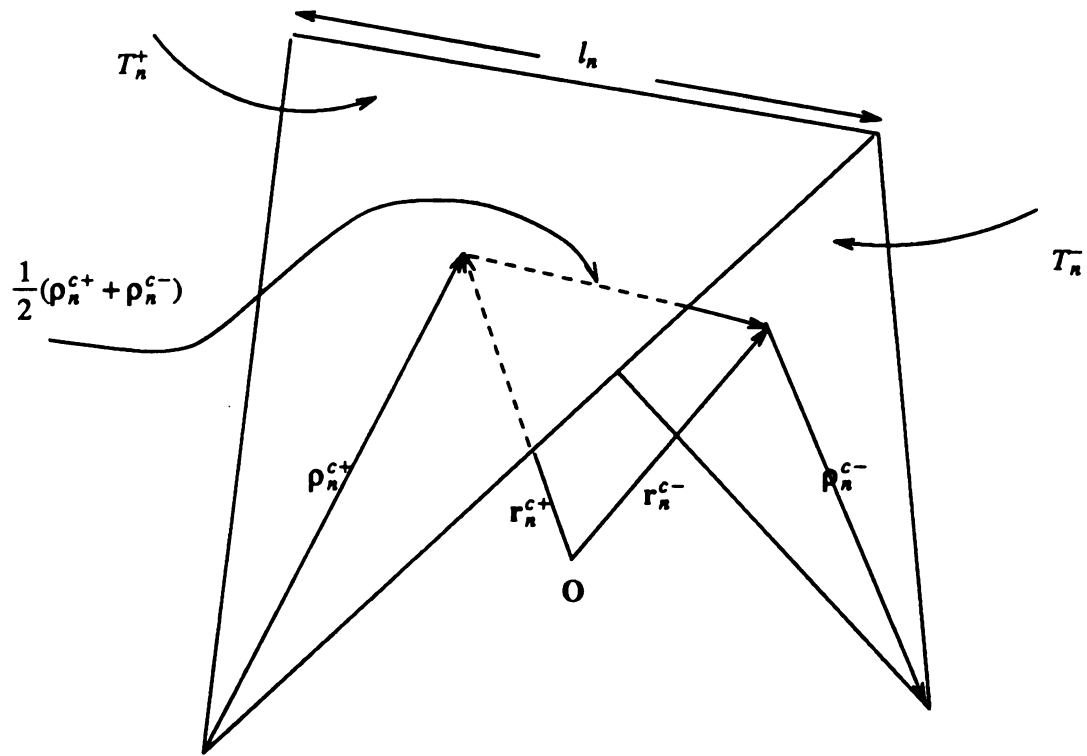
Fig.4. Geometry of vectors to centroids of triangles associated with an edge.

of S.

An important interpretation of (1.2) that follows from 1) and 3) is that the expansion coefficient I_n represents the normal component of $\hat{\mathbf{J}}(\mathbf{r})$ at the nth edge.

CHAPTER 2

Assumptions and Projection Method

Projection methods are a class of techniques for obtaining an approximate solution to an operator equation

$$T x = y , \qquad\qquad (2.1)$$

where $T: X \to X$ is a bounded linear operator with bounded inverse, X is a normed linear space. The approximate solution x_N of (2.1) is an element of a finite-dimensional subspace X_N of X satisfying

$$P_N T x_N = P_N y , \qquad\qquad (2.2)$$

where P_N is a bounded projection operator (a linear idempotent operator) on X with range X_N. From this general scheme we obtain the Galerkin method.

Now we want to develop a process yielding the approximate solution of our electric field integral equation by this method. First, we need the following preliminary assumptions:

1) In equation (2.1), $X = L^2(S)$, where S is a plate that can be modeled by triangular patches perfectly, i.e.,

$$L^2(S) = \left\{ \mathbf{x} : S \to \mathbb{C}^2, \int_S |\mathbf{x}(\mathbf{r})|^2 \, d\mathbf{r} < \infty \right\}.$$

X is a Hilbert space with the inner product

$$< \mathbf{x}, \mathbf{y} > = \int_S \mathbf{x}(\mathbf{r}) \cdot \overline{\mathbf{y}}(\mathbf{r}) \, d\mathbf{r}, \qquad \mathbf{x}, \mathbf{y} \in L^2(S).$$

The operator **T** is an operator of form

$$\mathbf{T} = \mathbf{E} + \mathbf{K},$$

where **E** is the identity operator and **K** is a completely continuous integral operator. Thus equation (2.1) becomes

$$(\mathbf{E} + \mathbf{K}) \mathbf{x} = \mathbf{y}, \qquad \mathbf{x}, \mathbf{y} \in L^2(S). \tag{2.3}$$

It is a Fredholm equation of the second kind. Here and throughout, $\| \ \|$ denotes the L^2 norm.

2)   There is no solution of the equation

$$\mathbf{T}\,\mathbf{x} = \mathbf{0}$$

other than $\mathbf{x} = \mathbf{0}$. It follows from the Fredholm Alternative that $\mathbf{T}^{-1}$ exists and is bounded. Therefore equation (2.3) is well-posed.

3)   For all the triangulations of S that we consider, there are constants c_0 and θ_0 with $0 < \theta_0 < \pi/2$, such that

$$l_i / l_j \leq c_0 \quad \text{and} \quad \theta_0 \leq \theta_i^{\ddagger} \leq \pi - \theta_0,$$

where l_i is the length of the ith edge, and $\theta_i^{\ddagger}$ is the angle in the triangle $T_i^{\ddagger}$ opposite

the ith edge. For each triangulation τ, let $l_\tau = \max_\tau l_i$. It follows that

$$\frac{1}{c_0} \cdot l_\tau \le l_i \le l_\tau \,,$$

$$\frac{\sin\theta_0}{2c_0^2} \cdot l_\tau^2 \le A_i^\ddagger \le l_\tau^2 \,, \tag{2.4}$$

where $A_i^\ddagger$ is the area of the triangle $T_i^\ddagger$.

4) First, let $\mathbf{G}_N$ be an $N{\times}N$ matrix with the inner product of the basis functions $< \mathbf{f}_i \,, \mathbf{f}_j >$ as its $(j,\ i)^{th}$ entry. It is easy to verify that

$$\mathbf{G}_N = l^2\,\Gamma_N \,, \tag{2.5}$$

where $l = l_\tau$, Γ_N is a positive definite matrix which depends only on the shape of triangular elements. Throughout the approximation process we attempt to keep the elements in the same shape. This means that we only change the size of the patches. The shape of elements is designed to satisfy

$$\delta_0 \le \min_{\lambda_i \in \sigma(\Gamma_N)} \lambda_i \le \max_{\lambda_i \in \sigma(\Gamma_N)} \lambda_i \le \tilde{\delta}_0 \quad \text{for all } N \,, \tag{2.6}$$
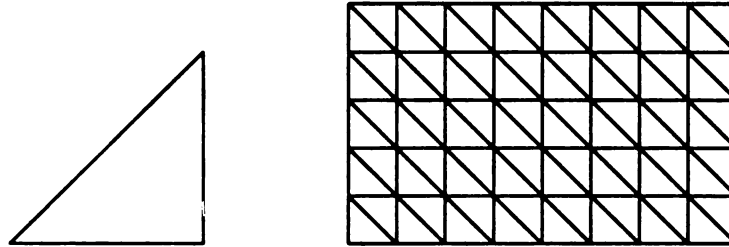
where δ_0, $\tilde{\delta}_0$ are some positive constants, and $\sigma(\Gamma_N)$ is the spectrum of the matrix Γ_N. Thus

$$cond\,(\Gamma_N) \le \tilde{\delta}_0 / \delta_0 \quad \text{for all } N \,, \tag{2.7}$$

where $cond\,(\Gamma_N)$ denotes the condition number of Γ_N. For example, $cond\,(\Gamma_N) \le 7/3$ and $cond\,(\Gamma_N) < 4$ if we choose triangles as shown in Fig.5 (a) and (b) respectively. We shall see in Chapter 4 that this is one of the conditions that guarantees the stability of the numerical computation.

.
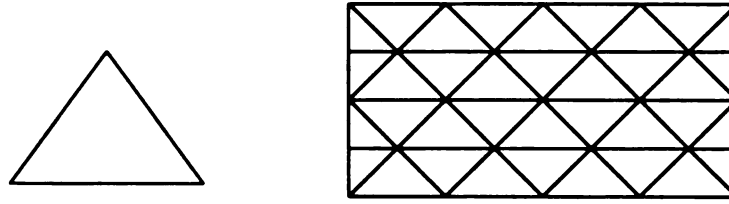
(a)

(b)

Fig.5. Design of triangular patches.

5) For a fixed triangulation τ, define

$$X_N = \left\{ \sum_{i=1}^{N} I_n f_n \mid I_n \ (n = 1,..., N) \text{ are complex numbers} \right\},$$

where N is the number of edges of the triangular model. X_N is an N-dimensional

linear subspace of $L^2(S)$. From previous assumptions, the projected equation(2.2) becomes

$$(E + P_N K) x_N = P_N y ,$$ (2.8)

where $y \in L^2(S)$, $x_N \in X_N$.

For the Galerkin method a specific projection operator P_N is defined as follows:

Definition. For each x in $L^2(S)$, let $P_N x = \sum_{n=1}^{N} I_n f_n$, where the coefficients $I = (I_1, \ldots, I_N)^T$ are determined by the solution of the linear system

$$G_N I = (< x , f_1 >, \ldots, < x , f_N >)^T .$$ (2.9)

Since G_N is a positive definite matrix, equation (2.9) has a unique solution for any $x \in L^2(S)$. Thus P_N is a well defined operator from $L^2(S)$ onto the N-dimensional subspace X_N. Also it is easy to verify that P_N is a projection with the properties:

(1) $< P_N x , f_m > = < x , f_m >$ ($m = 1,.., N$) for all $x \in L^2(S)$.

(2) $\| P_N \| \le 1$ for all N.

Let x^* denote the exact solution of equation (2.3). A projection method to approximate x^* proceeds as follows:

Choose an approximation $x_N = \sum_{n=1}^{N} I_n f_n \in X_N$, and determine its coefficients $\{I_i\}$ by requiring that $T x_N - y$ vanishes under the projection P_N. Let $ERR = T x_N - y$. From the definition of P_N, $P_N ERR = 0$ if and only if

$$< ERR , f_m > = 0 , \quad (m = 1,\ldots, N) .$$

Therefore the coefficients of x_N are determined by

$$< T x_N , f_m > = < y , f_m > , \quad (m = 1,\ldots, N) ,$$

that is

$$\mathbf{Z}_N \mathbf{I} = \mathbf{V}, \tag{2.10}$$

where $\mathbf{Z}_N$ is an $N \times N$ matrix with $< \mathbf{T} \mathbf{f}_i, \mathbf{f}_j >$ as its $(j, i)^{th}$ entry, $\mathbf{I} = (I_1, \dots, I_N)^T$ are coefficients of the approximation x_N, and $\mathbf{V} = (< y, \mathbf{f}_1 >, \dots, < y, \mathbf{f}_N >)^T$ is a vector with $< y, \mathbf{f}_i >$ as the ith component.

In order to analyze this process and give an error estimate of the approximate solution, we need the following theorem.

Theorem 2.1. $\mathbf{P}_N \mathbf{x} \to \mathbf{x}$ as $N \to \infty$ for all $\mathbf{x} \in L^2(S)$. In particular,

$$\| \mathbf{P}_N \mathbf{x} - \mathbf{x} \| = O(l), \quad \text{if } \mathbf{x} \in C^2(S), \tag{2.11}$$

where

$$C^2(S) = \left\{ \mathbf{x} : S \to \mathbf{C}^2, \ \mathbf{x} \text{ has continuous second derivatives.} \right\}$$

Proof. Using the property (1) of $\mathbf{P}_N$, for any $y \in X_N$,

$$< \mathbf{P}_N \mathbf{x} - \mathbf{x}, y > = < \mathbf{P}_N \mathbf{x}, y > - < \mathbf{x}, y >$$

$$= 0,$$

that is, $\mathbf{P}_N \mathbf{x} - \mathbf{x}$ is perpendicular to the subspace X_N. Therefore

$$\| \mathbf{P}_N \mathbf{x} - \mathbf{x} \| = dis(\mathbf{x}, X_N), \tag{2.12}$$

where $dis(\mathbf{x}, X_N) = \min_{x_N \in X_N} \| \mathbf{x} - x_N \|$. It is sufficient to show that

$$dis(\mathbf{x}, X_N) \to 0 \quad \text{as } N \to \infty.$$

Case 1, $x \in C^2(S)$ ($x \neq 0$):

Choose $x_N = \sum\limits_{i=1}^{N} I_i \, f_i$, where

$$I_i = x(r_i) \cdot n_i , \qquad (2.13)$$

r_i is an arbitrary point on the ith edge and n_i is a unit vector normal to the ith edge. Let the error function $e(r)$ be defined as

$$e(r) = x(r) - x_N(r) .$$

Inside a triangle T, we draw a small triangle T' with sides parallel to the sides of T and with vertices $\tilde{r}_i$ ($i = 1, 2, 3$). δ is the uniform width between T and T' which satisfies

$$0 < \delta < \frac{2 \min A_n^{\pm}}{3 \| x \|_\infty} \qquad (2.14)$$

and the Lebesgue measure of $S - \cup_i T'_i$ satisfies

$$meas \, (S - \cup_i T'_i) < l^2 . \qquad (2.15)$$

Here $\| x \|_\infty = \max\limits_{r \in S} | x(r) |$. Without loss of generality, T is labeled as shown in Fig.6.

At $r = \tilde{r}_1$,

$$e(\tilde{r}_1) \cdot n_2 = x(\tilde{r}_1) \cdot n_2 - \sum_{i=1}^{3} I_i \, f_i(\tilde{r}_1) \cdot n_2$$

$$= x(\tilde{r}_1) \cdot n_2 - \left[I_1 \, \frac{l_1}{2A} \, \delta_1 + I_2 \, \frac{l_2}{2A} \, (h_2 + \delta_2) + I_3 \, \frac{l_3}{2A} \, \delta_3 \right]$$

$$= x(\tilde{r}_1) \cdot n_2 - I_2 - \tilde{\delta} ,$$
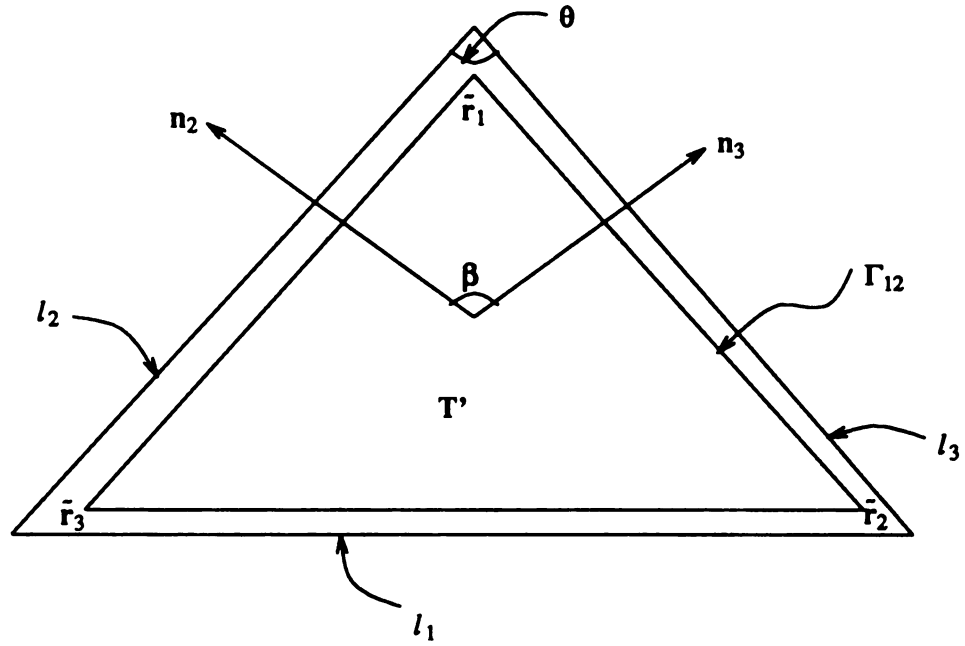
Fig.6. Triangle T and T'.

where $|\,\delta_i\,| = \delta$, A is the area of triangle T, and $\tilde{\delta} = \dfrac{1}{2A} \sum_{i=1}^{3} l_i\, l_i\, \delta_i$. From (2.13)

$$e(\tilde{r}_1) \cdot n_2 = x(\tilde{r}_1) \cdot n_2 - x(r_2) \cdot n_2 - \tilde{\delta}$$

$$= \int_0^1 \nabla x(r_2 + tz)\, z\, dt \cdot n_2 - \tilde{\delta}, \qquad \text{where } z = \tilde{r}_1 - r_2\ .$$

Using (2.14), yields

$$|\,e(\tilde{r}_1) \cdot n_2\,| \leq \|\,\nabla x\,\|_\infty \cdot l + l$$

$$= const \cdot l\ , \tag{2.16}$$

where $const = (\| \nabla x \|_\infty + 1)$ is independent of l. For simplicity, we shall use $const$ to denote constant numbers that are independent of l. Here and throughout, $const$'s may not have the same value. Similarly, we get

$$| e(\tilde{r}_1) \cdot n_3 | \le const \cdot l . \tag{2.17}$$

Let i, j be an orthonormal basis on S. Then there exist real numbers c_1 and c_2, such that

$$i = c_1 \, n_2 + c_2 \, n_3 .$$

Applying n_2, n_3 on both sides of this equation, we have

$$i \cdot n_2 = c_1 + n_3 \cdot n_2 \, c_2 ,$$

$$i \cdot n_3 = n_2 \cdot n_3 \, c_1 + c_2 .$$

The above two equations can be written as a matrix equation

$$\begin{bmatrix} 1 & n_2 \cdot n_3 \\ n_2 \cdot n_3 & 1 \end{bmatrix} \begin{bmatrix} c_1 \\ c_2 \end{bmatrix} = \begin{bmatrix} i \cdot n_2 \\ i \cdot n_3 \end{bmatrix} .$$

Let β be the angle between n_2 and n_3. From assumption 3) and Fig.6,

$$(n_2 \cdot n_3)^2 = \cos^2\beta = \cos^2\theta_1 \le \cos^2\theta_0 .$$

Thus the determinant of the above coefficient matrix

$$\det \begin{bmatrix} 1 & n_2 \cdot n_3 \\ n_2 \cdot n_3 & 1 \end{bmatrix} = 1 - (n_2 \cdot n_3)^2$$

$$\ge 1 - \cos^2\theta_0 > 0 .$$

It follows from Cramer's Rule that

$$| c_i | \le const \qquad i = 1, 2.$$

Here, *const* is independent of triangular elements. Therefore

$$| e(\tilde{r}_1) \cdot \mathbf{i} | = | c_1 e(\tilde{r}_1) \cdot \mathbf{n}_2 + c_2 e(\tilde{r}_1) \cdot \mathbf{n}_3 | \le const \cdot l$$

by (2.16) and (2.17). Similarly, we obtain

$$| e(\tilde{r}_1) \cdot \mathbf{j} | \le const \cdot l .$$

Thus

$$| e(\tilde{r}_1) | = \sqrt{| e(\tilde{r}_1) \cdot \mathbf{i} |^2 + | e(\tilde{r}_1) \cdot \mathbf{j} |^2} \le const \cdot l .$$

Repeating this process, we get

$$| e(\tilde{r}_i) | \le const \cdot l , \quad i = 1, 2, 3, \tag{2.18}$$

where each *const* depends only on $\| \nabla x \|_\infty$ and is proportional to c_0.

Next we are going to show that (2.18) holds for all points on the edges of T':

$$\Gamma_{i,j} = \left\{ \mathbf{r} \mid \mathbf{r} = \tilde{r}_i + t (\tilde{r}_j - \tilde{r}_i), \ t \in [0, 1] \right\}, \quad (i, j) \in \left\{ (1, 2), (1, 3), (2, 3) \right\}.$$

Once this is proved, (2.18) will be true for all the points of the segments which have end points on those edges. Therefore

$$| e(\mathbf{r}) | \le const \cdot l , \quad \text{for all } \mathbf{r} \in T'_i, i = 1, 2, ..., n_T , \tag{2.19}$$

here n_T is the number of triangles. We shall see that *const* here depends only on $\| D^\alpha x \|_\infty$ ($| \alpha | \le 2$) and c_0 .

It is sufficient to prove (2.18) on edge $\Gamma_{1,2}$. On $\Gamma_{1,2}$, there is a point $r_0 = \tilde{r}_1 + t_0(\tilde{r}_2 - \tilde{r}_1)$ ($t_0 \in [0, 1]$), such that

$$| e(r_0) | = \max_{r \in \Gamma_{1,2}} | e(r) | .$$

Without loss of generality, we assume that $| e(r_0) | > 0$. We let

$$n_0 = \frac{e(r_0)}{| e(r_0) |}$$

and

$$g(t) = e(\tilde{r}_1 + t (\tilde{r}_2 - \tilde{r}_1)) \cdot n_0 , \quad t \in [0, 1] .$$

Since $g \in C^2[0,1]$ and $g(t_0)$ is an extrema,

$$g(0) = g(t_0) + \frac{g''(\xi)}{2} (-t_0)^2 , \quad \text{for some } \xi \in [0, 1] .$$

Consequently

$$| e(r_0) | = | g(t_0) | \le | g(0) | + \frac{1}{2} | g''(\xi) |$$

$$\le | e(\tilde{r}_1) \cdot n_0 | + const \cdot M \cdot | \tilde{r}_2 - \tilde{r}_1 |^2$$

$$\le const \cdot l + const \cdot M \cdot l^2 ,$$

where $M = \max_{r \in S, |\alpha|=2} | D^\alpha x(r) |$. Thus

$$| e(r) | \le const \cdot l , \quad \text{for all } r \in \Gamma_{1,2} .$$

It is easy to see that (2.19) can be proved by using the same technique. Now,

$$\| e \|^2 = \int_S | e(r) |^2 \, dr$$

$$= \int_{\cup T_i} | e(r) |^2 \, dr + \int_{S-\cup T_i} | e(r) |^2 \, dr$$

$$\leq const \cdot l^2 + 2 \left[\int_{S-\cup T_i} | x(r) |^2 \, dr + \int_{S-\cup T_i} | x_N(r) |^2 \, dr \right] \quad \text{by (2.19)}$$

$$\leq const \cdot l^2 + 2 \left[\| x \|_\infty^2 + (3 \| x \|_\infty \max_i \| f_i \|_\infty)^2 \right] meas(S - \cup T_i)$$

$$\leq const \cdot l^2 \quad \text{by (2.4) and (2.15).}$$

Hence,

$$dis(x , X_N) \leq \| e \| \leq const \cdot l ,$$

where *const* depends only on $\| D^\alpha x \|_\infty$ ($| \alpha | \leq 2$) and is proportional to c_0.

Case 2, $x \in L^2(S)$:

Since $C^2(S)$ is dense in $L^2(S)$, there exists a sequence $\{ x^{(m)} \}$ in $C^2(S)$, such that $x^{(m)} \to x$ in L^2 norm as $m \to \infty$. For any $\varepsilon > 0$, choose $x^{(m)}$ satisfying $\| x - x^{(m)} \| < \varepsilon/2$. Then

$$dis(x , X_N) \leq \| x - x^{(m)} \| + dis(x^{(m)} , X_N)$$

$$< \varepsilon/2 + const \cdot l .$$

Fixing $x^{(m)}$ and choosing N sufficiently large(this is equivalent to l is small enough), we obtain

$$dis(\mathbf{x}, \mathbf{X}_N) < \varepsilon.$$

This proves that $dis(\mathbf{x}, \mathbf{X}_N) \to 0$ as $N \to \infty$. $\square$

CHAPTER 3

Convergence and Error Bound

In this chapter, we show that the projection method defined by a subspace X_N and an operator P_N determines a unique solution of the linear system (2.10), which then gives an approximate solution x_N of the integral equation (2.1). The sequence { x_N } converges to the exact solution x^* of (2.1) as the diameters of elements tend to zero uniformly. Moreover, the error bound can be found and the method gives a first order approximation if x^* is smooth enough.

Let the operator K and projections {P_N} be defined as in chapter 2. We denote $H_N = E + P_N K$ and $\overline{H}_N = H_N|_{X_N}$. Here $\overline{H}_N$ is the restriction of H_N on subspace X_N. Then equation (2.8) can be written as

$$\overline{H}_N x_N = P_N y . \tag{3.1}$$

This equation is uniquely solvable for any $y \in L^2(S)$ if and only if $\overline{H}_N^{-1}$ exists. Since {H_N} converges to T, which is invertible and its inverse is bounded, the existence of H_N^{-1} and $\overline{H}_N^{-1}$ is guaranteed by the following lemma and theorem:

Lemma 3.1. $\| P_N K - K \| \to 0$ as $N \to \infty$.

Proof. The assertion follows from theorem 2.1 and lemma 2 in [2, pg.53]. $\square$

Theorem 3.2. Let X be a Banach space and $L(X)$ the normed vector space of bounded linear operators from X into X. Suppose $L, L_0, L_0^{-1} \in L(X)$. If

$\Delta = \| L - L_0 \| \| L_0^{-1} \| < 1$, then $L^{-1} \in L(X)$ and

$$L^{-1} = [\sum_{n=0}^{\infty} (L_0^{-1} (L_0 - L))^n] L_0^{-1} .$$

Proof. See [3, pg.87]. □

Lemma 3.1 enables us to choose N_0, such that

$$q_N = \| P_N K - K \| \| T^{-1} \| < 1, \quad \text{if } N > N_0 . \tag{3.2}$$

Using theorem 3.2, H_N^{-1} exists when $N > N_0$ and

$$H_N^{-1} = [\sum_{n=0}^{\infty} (T^{-1} (K - P_N K))^n] T^{-1} .$$

Then we have the inequality

$$\| H_N^{-1} \| \le \frac{1}{1 - q_N} \| T^{-1} \| , \quad \text{when } N > N_0 . \tag{3.3}$$

Since equation (3.1) is uniquely solvable for any $y \in L^2(S)$ if and only if the linear system (2.10) is uniquely solvable, the matrix Z_N is nonsingular if $N > N_0$. This proves the feasibility of the approximation procedure.

In order to prove the convergence and give an error analysis, we apply P_N on both sides of (2.3):

$$P_N(E + K)x^* = P_N y .$$

Using (2.8), we find that

$$H_N(x^* - x_N) = x^* - P_N x^* .$$

From(3.3), we get

$$\| x^* - x_N \| \leq \| H_N^{-1} \| \, \| x^* - P_N x^* \|$$

$$\leq \frac{1}{1 - q_N} \| T^{-1} \| \, \| x^* - P_N x^* \| \quad \text{if } N > N_0 \, .$$

Applying theorem 2.1 and lemma 3.1, yields

$$\| x^* - x_N \| \to 0 \, , \quad \text{as } N \to \infty \, ,$$

where x_N is the unique solution of (3.1) and its coefficients are determined by the solution of matrix equation (2.10). Moreover, from theorem 2.1 we have the error bound

$$\| x^* - x_N \| \leq const \cdot l \, , \quad \text{if } x^* \in C^2(S) \, .$$

Here the constant number $const$ depends only on $\| D^\alpha x^* \|_\infty$ ($| \alpha | \leq 2$) and is proportional to c_0 defined in chapter 2.

CHAPTER 4

Computational Stability

The approximated solution x_N is determined in terms of the basis functions $\{f_n\}$ of subspace X_N used in the computational scheme. To examine the influence of these basis functions on the stability of the linear system

$$Z_N I = V,\tag{4.1}$$

we have the following theorem:

Theorem 4.1. The condition number of the matrix Z_N of (4.1) satisfies the inequality

$$cond(Z_N) \leq const \cdot cond(G_N) \quad \text{when } N \text{ is large enough.}\tag{4.2}$$

Here *const* is a constant number independent of N, and G_N is an $N \times N$ matrix defined in assumption 4) of chapter 2.

Proof. Let C be the set of all complex numbers, and $\Phi : X_N \to C^N$ be defined by

$$\Phi(x) = (<x, f_1>,...,<x, f_N>)^T, \quad \text{for all } x \in X_N,$$

i.e., if $x_N = \sum_{i=1}^{N} I_i f_i \in X_N$, then

$$\Phi(x) = G_N I,\tag{4.3}$$

with $\mathbf{I} = (I_1, I_2, \cdots, I_N)^T$. Since $\mathbf{G}_N$ is invertible, Φ is invertible. Moreover, for any $\mathbf{x}_N \in \mathbf{X}_N$, we have

$$\| \Phi(\mathbf{x}_N) \|^2 = \sum_{i=1}^{N} | < \mathbf{x}_N , \mathbf{f}_i > |^2$$

$$\leq \sum_{i=1}^{N} (\| \mathbf{f}_i \|^2 \int_{T_i^+ \cup T_i^-} | \mathbf{x}_N(\mathbf{r}) |^2 \, d\mathbf{r})$$

$$\leq (\max_i \| \mathbf{f}_i \|^2)(\sum_{i=1}^{N} \int_{T_i^+ \cup T_i^-} | \mathbf{x}_N(\mathbf{r}) |^2 \, d\mathbf{r})$$

$$\leq (\max_i \| \mathbf{f}_i \|^2)(3 \| \mathbf{x}_N \|^2) .$$

Since

$$\| \mathbf{f}_i \|^2 = \int_S | \mathbf{f}_i |^2 \, d\mathbf{r}$$

$$= \int_{T_i^+} | \mathbf{f}_i |^2 \, d\mathbf{r} + \int_{T_i^-} | \mathbf{f}_i |^2 \, d\mathbf{r}$$

$$\leq \left[\frac{l_i^2}{4 A_i^+} + \frac{l_i^2}{4 A_i^-} \right] l^2$$

$$\leq const \cdot l^2 \quad \text{by (2.4)}.$$

Thus

$$\| \Phi \| \leq const \cdot l . \tag{4.4}$$

On the other hand, for any $c \in C^N$, there exists an $x_N = \sum_{i=1}^{N} I_i f_i \in X_N$, such that

$$c = \Phi(x_N) = G_N I. \tag{4.5}$$

Using assumption 4) of chapter 2, we obtain

$$\| \Phi^{-1}(c) \|^2 = \| x_N \|^2$$

$$= \| \sum_{i=1}^{N} I_i f_i \|^2$$

$$= I^* G_N I$$

$$= (G_N^{-1} c)^* G_N (G_N^{-1} c) \quad \text{by (4.5)}.$$

That is

$$\| \Phi^{-1}(c) \|^2 = c^* G_N^{-*} c$$

$$= \frac{1}{l^2} c^* \Gamma_N^{-*} c$$

$$\leq \frac{1}{l^2} \| \Gamma_N^{-1} \| \| c \|^2$$

$$\leq \frac{1}{l^2} \frac{1}{\delta_0} \| c \|^2 \quad \text{by (2.6)}$$

$$= \frac{const}{l^2} \| c \|^2 .$$

Here $const(= \frac{1}{\delta_0})$ is independent of N. Thus

$$\| \Phi^{-1} \| \le const / l \ . \tag{4.6}$$

Next, applying Φ to (3.1) and noting that

$$\mathbf{Z}_N \ \mathbf{I} = \Phi \ (\mathbf{P}_N \ \mathbf{y}) \ ,$$

we find

$$\mathbf{Z}_N \ \mathbf{I} = \Phi \ \overline{\mathbf{H}}_N \ \mathbf{x}_N$$

$$= \Phi \ \overline{\mathbf{H}}_N \ (\Phi^{-1} \ \mathbf{G}_N \ \mathbf{I}) \quad \text{for any } \mathbf{I} \in \mathbf{C}^N \ .$$

This implies that

$$\mathbf{Z}_N = \Phi \ \overline{\mathbf{H}}_N \ \Phi^{-1} \ \mathbf{G}_N \ .$$

Thus we obtain

$$cond(\mathbf{Z}_N) = \| \mathbf{Z}_N \| \cdot \| \mathbf{Z}_N^{-1} \|$$

$$\le (\| \Phi \| \ \| \Phi^{-1} \| \ )^2 \| \mathbf{H}_N \| \ \| \mathbf{H}_N^{-1} \| \ cond(\mathbf{G}_N)$$

$$\le const \cdot cond(\mathbf{G}_N) \quad \text{if } N > N_0 \ ,$$

where N_0 is the positive integer used in the inequality (3.2). $\square$

Using assumption 4) of chapter 2, we have

$$cond(\mathbf{G}_N) \le \tilde{\delta}_0 / \delta_0 \quad \text{for all } N \ .$$

Therefore the numerical scheme is stable as $N \to \infty$.

The bound (4.2) suggests that we should design triangles with considerable caution to make $cond(\mathbf{G}_N)$ as small as possible. Also, the modulus of operators $\mathbf{E} + \mathbf{K}$ and

$(E + K)^{-1}$ will influence the stability of the scheme. With small modulus, we may expect more accurate approximation.

CHAPTER 5

Numerical Results

In this chapter we demonstrate the formulation of coupled surface integral equations(CSIE) and corresponding matrix equation. Then the numerical results are presented for the case of a homogeneous dielectric sphere in free space and excited by a plane wave.

5.1 The formulation of coupled surface integral equations

The detailed derivation of the coupled surface integral equations can be found in [4] and [5], but for completeness and further numerical development only a summary of the CSIE equations is given below. Referring to Fig.7, S denotes the surface of a homogeneous, lossy dielectric scatterer having a volume V contained in region 2 and bounded by the surface S. The scatterer is located in region 1 representing an isotropic, lossless free space medium. Let

$$(E_1^s, H_1^s) = \text{scattered electric and magnetic fields in region 1}$$

$$(E_2^s, H_2^s) = \text{scattered electric and magnetic fields in region 2}.$$

Then, referring to the electromagnetic equivalent principle, various scattered electric
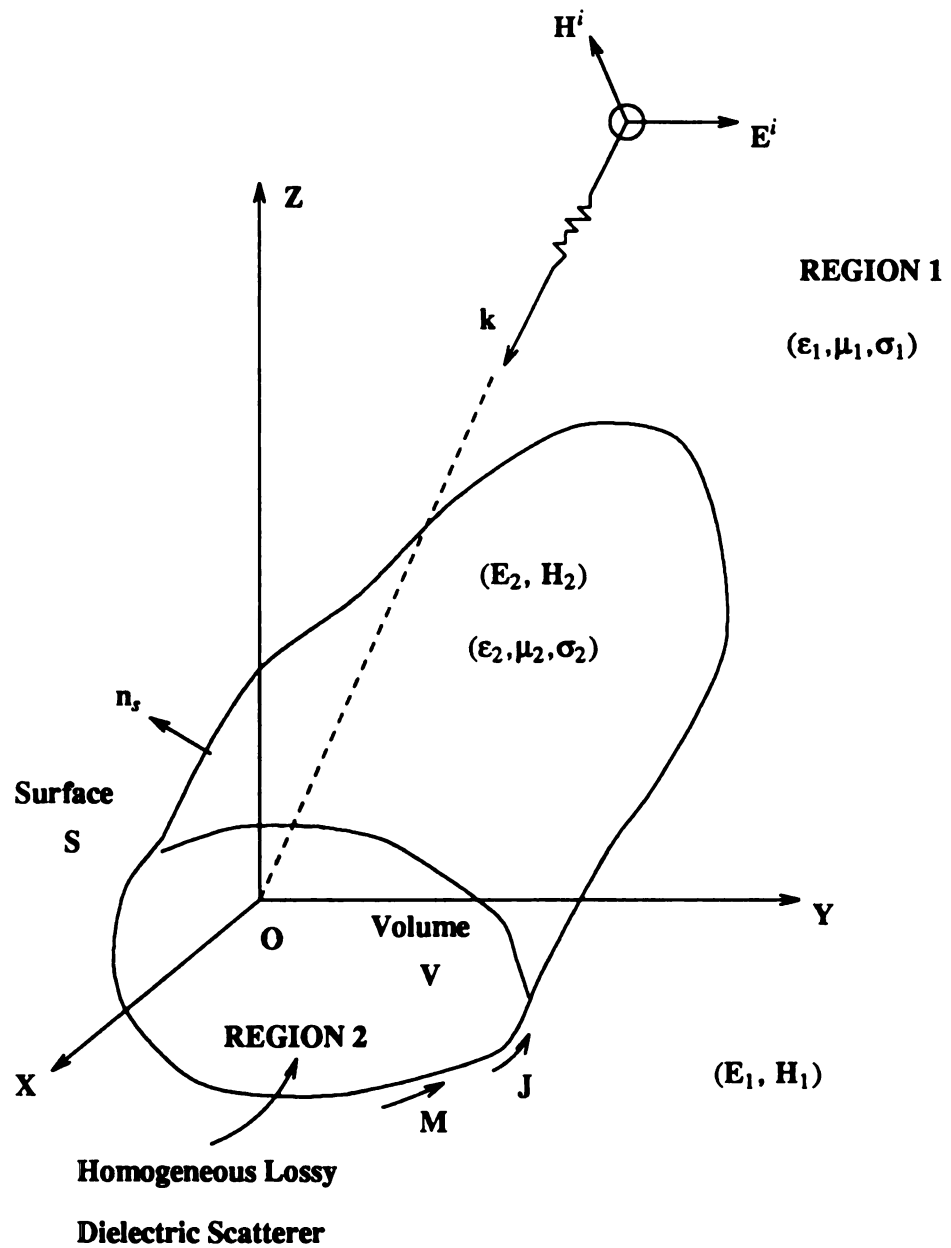
Fig.7. Geometry of a homogeneous lossy dielectric

scatterer in an isotropic free space medium.

and magnetic fields in regions 1 and 2 are given by

$$\mathbf{E}_1^s(\mathbf{r}) = -j\omega\mathbf{A}_1(\mathbf{r}) - \nabla V_1(\mathbf{r}) - \frac{1}{\varepsilon_1'}\nabla\times\mathbf{F}_1(\mathbf{r}) \qquad (5.1.1)$$

$$\mathbf{H}_1^s(\mathbf{r}) = -j\omega\mathbf{F}_1(\mathbf{r}) - \nabla U_1(\mathbf{r}) + \frac{1}{\mu_1}\nabla\times\mathbf{A}_1(\mathbf{r}), \quad \text{for } \mathbf{r} \text{ on or outside } S \qquad (5.1.2)$$

$$\mathbf{E}_2^s(\mathbf{r}) = j\omega\mathbf{A}_2(\mathbf{r}) + \nabla V_2(\mathbf{r}) + \frac{1}{\varepsilon_2'}\nabla\times\mathbf{F}_2(\mathbf{r}) \qquad (5.1.3)$$

$$\mathbf{H}_2^s(\mathbf{r}) = j\omega\mathbf{F}_2(\mathbf{r}) + \nabla U_2(\mathbf{r}) - \frac{1}{\mu_2}\nabla\times\mathbf{A}_2(\mathbf{r}), \quad \text{for } \mathbf{r} \text{ on or inside } S \qquad (5.1.4)$$

where the various vector potentials $\mathbf{A}_i$ and $\mathbf{F}_i$ and the scalar potentials V_i, and U_i, for $i = 1, 2$ are given by

$$\mathbf{A}_i(\mathbf{r}) = \frac{\mu_i}{4\pi} \iint_S \mathbf{J}(\mathbf{r}\prime)G_i(\mathbf{r}, \mathbf{r}\prime)\, dS(\mathbf{r}\prime) \qquad (5.1.5)$$

$$\mathbf{F}_i(\mathbf{r}) = \frac{\varepsilon_i'}{4\pi} \iint_S \mathbf{M}(\mathbf{r}\prime)G_i(\mathbf{r}, \mathbf{r}\prime)\, dS(\mathbf{r}\prime) \qquad (5.1.6)$$

$$V_i(\mathbf{r}) = \frac{1}{4\pi\varepsilon_i'} \iint_S \rho^e(\mathbf{r}\prime)G_i(\mathbf{r}, \mathbf{r}\prime)\, dS(\mathbf{r}\prime) \qquad (5.1.7)$$

$$U_i(\mathbf{r}) = \frac{1}{4\pi\mu_i} \iint_S \rho^m(\mathbf{r}\prime)G_i(\mathbf{r}, \mathbf{r}\prime)\, dS(\mathbf{r}\prime) \qquad (5.1.8)$$

$$\varepsilon_i' = \varepsilon_i \left[1 - j\frac{\sigma_i}{\omega\varepsilon_i} \right] \qquad (5.1.9)$$

and

$$\rho^e(\mathbf{r}\prime) = \frac{-1}{j\omega} [\, \nabla_{s}\prime \cdot \mathbf{J}(\mathbf{r}\prime) \,] \qquad (5.1.10)$$

$$\rho^m(r\prime) = \frac{-1}{j\omega} [\nabla_{s\prime} \cdot M(r\prime)].$$

(5.1.11)

In obtaining the above expressions, $e^{j\omega t}$ time dependence is assumed for various field quantities and ω is the frequency in radians per second. The Green's function defined in (5.1.5)-(5.1.8) for $i = 1, 2$ is given by

$$G_i(r, r\prime) = \frac{e^{jk_iR}}{R}$$

(5.1.12)

$$R = | r - r\prime |$$

(5.1.13)

and the propagation constant is

$$k_i = [\omega^2 \mu_i \epsilon_{i\prime}]^{\frac{1}{2}}.$$

(5.1.14)

In (5.1.5) and (5.1.6), J is the equivalent electric current and M is the equivalent magnetic current on the surface of the dielectric scatterer. The equivalent electric and magnetic currents are, in fact, related to the surface total magnetic and electric fields tangential to the surface S:

$$J(r\prime) = n_s \times H(r\prime)$$

(5.1.15)

$$M(r\prime) = E(r\prime) \times n_s, \quad r\prime \text{ on the surface } S$$

(5.1.16)

where n_s is an outward unit normal on S shown in Fig.7. Further, in the above expressions, $(\epsilon_1, \mu_1, \sigma_1 = 0)$ and $(\epsilon_2, \mu_2, \sigma_2)$ are the permittivity, permeability, and conductivity for the regions 1 and 2.

On enforcing the boundary condition that the total tangential electric field and the total tangential magnetic field should be continuous across the surface of the arbitrary dielectric scatterer, the following coupled surface integral equations are obtained in terms of the unknown surface equivalent electric and magnetic currents:

$$\mathbf{E}^i(\mathbf{r})\big|_{tan} = \{ \, j\omega[\, \mathbf{A}_1(\mathbf{r}) + \mathbf{A}_2(\mathbf{r}) \,] + [\, \nabla V_1(\mathbf{r}) + \nabla V_2(\mathbf{r}) \,]$$

$$+ \nabla \times \left[\frac{\mathbf{F}_1(\mathbf{r})}{\varepsilon_1{'}} + \frac{\mathbf{F}_2(\mathbf{r})}{\varepsilon_2{'}} \right] \}\big|_{tan} \qquad (5.1.17)$$

$$\mathbf{H}^i(\mathbf{r})\big|_{tan} = \{ \, j\omega[\mathbf{F}_1(\mathbf{r}) + \mathbf{F}_2(\mathbf{r})] + [\, \nabla U_1(\mathbf{r}) + \nabla U_2(\mathbf{r}) \,]$$

$$- \nabla \times \left[\frac{\mathbf{A}_1(\mathbf{r})}{\mu_1} + \frac{\mathbf{A}_2(\mathbf{r})}{\mu_2} \right] \}\big|_{tan} , \qquad \mathbf{r} \text{ on surface } S \qquad (5.1.18)$$

where $\mathbf{E}^i$ and $\mathbf{H}^i$ are the incident electric and magnetic fields in region 1 and the subscript "tan" refers to tangential component. Thus, coupled surface integral equations in general can be expressed as

$$T_{11}\mathbf{J}(\mathbf{r}) + T_{12}\mathbf{M}(\mathbf{r}) = \mathbf{E}^i(\mathbf{r}) \qquad (5.1.19)$$

$$T_{21}\mathbf{J}(\mathbf{r}) + T_{22}\mathbf{M}(\mathbf{r}) = \mathbf{H}^i(\mathbf{r}) \qquad (5.1.20)$$

for $\mathbf{r} \in S$, where T_{ij} are linear integral operators, $\mathbf{J}$, $\mathbf{M}$ are equivalent electric and magnetic surface current, $\mathbf{E}^i$, $\mathbf{H}^i$ are incident electric and magnetic fields respectively, and S is a regular two dimensional region of interest. Set

$$T = \begin{bmatrix} T_{11} & T_{12} \\ T_{21} & T_{22} \end{bmatrix}$$

$$\tilde{\mathbf{J}}(\mathbf{r}) = [\, \mathbf{J}(\mathbf{r}) , \, \mathbf{M}(\mathbf{r}) \,]^T$$

$$\tilde{\mathbf{E}}(\mathbf{r}) = [\, \mathbf{E}^i(\mathbf{r}) , \, \mathbf{H}^i(\mathbf{r}) \,]^T .$$

Equations (5.1.19) and (5.1.20) then become

$$T \tilde{J}(r) = \tilde{E}(r) \quad r \in S .$$

Under appropriate assumptions, the theoretical analysis demonstrated in the previous chapters can be extended to certain types of coupled surface integral equations.

5.2 Matrix equation

Referring to the dielectric scatterer shown in Fig.1, the surface electric and magnetic current, **J** and **M**, distributions are expanded in terms of vector basis functions defined in chapter 1. Let N represents the total number of edges. Then the testing functions are written as

$$J(r\prime) = \sum_{n=1}^{N} I_n f_n(r\prime) \tag{5.2.1}$$

$$M(r\prime) = \sum_{n=1}^{N} M_n f_n(r\prime) \tag{5.2.2}$$

where I_n and M_n are coefficients yet to be determined. Since the normal component of f_n at the nth common edge connecting T_n^+ and T_n^- is unity, each coefficient of I_n and M_n can be interpreted as the normal components of the electric and magnetic current density flowing past the nth common edge.

In order to find the current coefficients, the coupled integral equations (5.1.19) and (5.1.20) are tested with respect to testing functions. The electric current and magnetic current expansion terms defined in (5.2.1) and (5.2.2) are now substituted into (5.1.19)-(5.1.20) and test the equations based on L^2 inner product. Hence, we obtain the matrix equation

$$< T_{11}J \, , \, f_m > + \, < T_{12}M \, , \, f_m > = \, < E^i \, , \, f_m > \qquad (5.2.3)$$

$$< T_{21}J \, , \, f_m > + \, < T_{22}M \, , \, f_m > = \, < H^i \, , \, f_m > \qquad (5.2.4)$$

for $m = 1,...,$ N. For the detailed numerical evaluation of matrix elements, the reader may refer to [6].

5.3 Numerical results

Although the coupled surface integral equations shown in section 5.1 are not second kind Fredholm equations as we assumed in previous chapters, the numerical
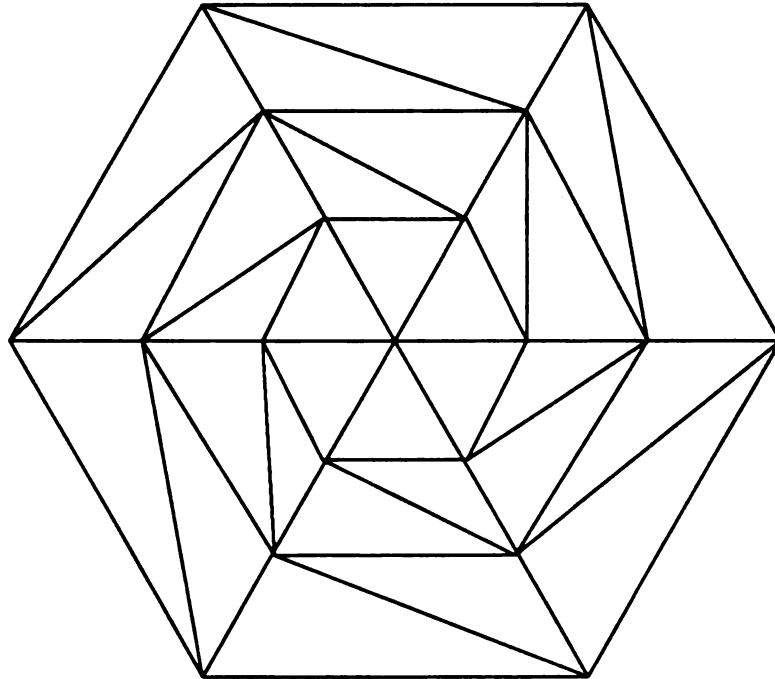
Fig.8. Triangular surface patching for

top half of sphere (plane view).

Table 1

ϕ	M_ϕ	
	Numerical Solution	Exact Solution
0.261799	0.771489	0.867912
0.785398	0.625174	0.710197
1.308997	0.455707	0.503564
1.832596	0.426590	0.461907
2.356194	0.530623	0.578552
2.879793	0.613626	0.670465
Error($e^{(1)}$)	6.53093e-02	

No. of faces = 60; No. of edges = 90;

Matrix size = 180×180; Mesh size($l^{(1)}$) = $2\pi/6$.

results show that the convergence rate is very close to our estimation. We shall present the experimental results for the case of a homogeneous dielectric sphere in free space and excited by a plane wave.

As we know, the sphere is not amenable to planar triangular modeling. Assuming that the geometrical discretization error can be decreased by reducing the size of the elements and such misfits are ignorable if the size of the elements is small enough, the surface of the sphere is modeled in terms of triangles having arbitrary edges and vertices arranged to depict the shape of a sphere. Fig.8 shows the plan view (top hemisphere

Table 2

φ	M_ϕ	
	Numerical Solution	Exact Solution
0.196350	0.818644	0.877422
0.589049	0.731751	0.783832
0.981748	0.584576	0.628048
1.374447	0.458582	0.485250
1.767146	0.433632	0.454231
2.159845	0.504070	0.530279
2.552544	0.592780	0.621703
2.945243	0.639877	0.675944
Error($e^{(2)}$)	3.87571e-02	

No. of faces = 112; No. of edges = 168;

Matrix size = 336×336; Mesh size($l^{(2)}$) = $2\pi/8$.

only) of the triangular scheme adopted. In our experiments, the electrical size of the sphere is $k_1 a = 1$ where the free space propagation constant $k_1 = 2\pi/\lambda_0$ and the radius of the sphere is a. The relative dielectric constant of the sphere is $\varepsilon_r = 4$. The sphere is located in free space and is excited by an axial incident plane wave. Table 1 and Table 2 show the numerical results of the induced magnetic current on the surface of the sphere along a circumferential arc in xz plane. Along the arc, there are two components of the

Table 3

Ratio	Error($e^{(2)} / e^{(1)}$)	0.593439
	Mesh Size($l^{(2)} / l^{(1)}$)	0.750000

magnetic current M_θ and M_ϕ. The results of the induced magnetic current are shown normalized with respect to incident electric field.

The ratio of the errors (e_2/e_1) and the corresponding ratio of mesh sizes are shown in Table 3. The experiments show that the convergence rate is at least linear. It is a little better than our estimation. This may be caused by the geometrical discretization error, the numerical integration of matrix elements and linear system solver. We have not taken into account these errors in our analysis. Since the basis functions are linear inside the patches and discontinuous on the edges, it is difficult to expect that the Galerkin method on such basis functions can achieve higher a convergence rate than linear convergence.

SUMMARY

The Galerkin method with new vector basis functions has been used by researchers in electrical engineering. Many experiments show that the new vector basis functions are ideally suited for representing surface electric current J and surface magnetic current M on the triangulated surface of the given dielectric scatterer. Efficient and simple numerical algorithms have been developed. In this work, a theoretical analysis on the convergence, error estimate and numerical stability of this method is given for certain type of electric field integral equations. More specifically, we are concerned with Fredholm integral equations of the second kind:

$$(E + K) J(r) = E^{i}(r) , \quad J, E^{i} \in L^{2}(S) ,$$

where E is the identity operator and K is a completely continuous integral operator. This restriction is sufficient but not necessary. If the integral equation $T J(r) = E^{i}(r)$ is well posed on $L^{2}(S)$ or on a subspace of $L^{2}(S)$ which contains $\bigcup_{N=1}^{\infty} X_{N}$, that is, the integral operator T is invertible and its inverse operator is bounded on the image of T, and in addition $P_{N}(T - E) \to T - E$ as $N \to \infty$, then all the results of this work still hold. In practice the physical properties of electric field integral equations may provide the first condition, while the second condition is not easy or practically is impossible to verify. In chapter 5, The numerical results of the coupled surface integral equations on a homo-

geneous dielectric sphere suggest that the convergence rate is at least linear, which confirms our estimation. The analysis of the Galerkin method with vector basis functions for general integral equations, especially for integral equations of the first kind remains an open question.

.

BIBLIOGRAPHY

BIBLIOGRAPHY

[1]   A. W. GLISSON, *On the Development of Numerical Techniques for Treating Arbitrarily-Shaped Surfaces.* Ph.D. dissertation, Univ. of Mississippi, 1978

[2]   K. E. ATKINSON, *A Survey of Numerical Method for the Solution of Fredholm Integral Equations of* the Second Kind. Society for Industrial and Applied Mathematics, 1976.

[3]   V. HUTSON AND J. S. PYM, *Applications of Functional Analysis and Operator Theory.* Academic Press Inc. (London) LTD. 1980.

[4]   K. R. UMASHANKAR AND A. TAFLOVE, *Analytical Models for Electromagnetic Scattering.* Part-I, Final Rep., Contract F19628-82-C-0140 to RADC/ESD, Hanscom Air Force Base, MA, June 1984.

[5]   J. R. MAUTZ AND R. F. HARRINGTON, *Electromagnetic Scattering From a Homogeneous Material Body of Revolution.* Arch. Elek. Ubertragung, vol. 33, no.4, pp.71-80, Apr. 1979.

[6]   K. R. UMASHANKAR, A. TAFLOVE AND S. M. RAO, *Electromagnetic Scattering by Arbitrary Shaped Three-Dimensional Homogeneous Lossy Dielectric Objects.* IEEE Transactions on Antennas and Propagation, vol. AP-34, no.6, June 1986.